doi: 10.4149/gpb_2023034

Inactivation of the TGF-β1/ALK5 axis enhances club cell function and alleviates lung tissue damage to ameliorate COPD progression through the MEK/ERK signaling pathway

Jing Tian[1], Hui Ouyang[1], Jie Wu[1], Lu Wen[1], Xiaoping Li[1], Fangying Yang[1] and Hao Yuan[1]

[1] *Pulmonary and Critical Care Medicine, Changsha Fourth Hospital, Changsha, Hunan, China*

Abstract. Chronic obstructive pulmonary disease (COPD) is a highly prevalent and fatal disease worldwide. The function of club cells, which are considered progenitor/stem cells of the bronchial epithelium, and their secreted protein CC16, have been proposed as potential targets for COPD treatment. This study aimed to investigate the role of the TGF-β1/ALK5 signaling pathway in club cell function and COPD progression. C57BL/6J mice were divided into Normal group (exposed to fresh air) and COPD group (exposed to incremental cigarette smoke extract for 12 weeks). The COPD mice were further divided into COPD group, DMSO group, and LY2109761 group (injected with 150 mg/kg LY2109761, a TGF-β1 inhibitor). Tissue staining was used to assess lung damage, and the expression of CC16 was measured. The levels of inflammatory factors and DNA damage-related indicators were also measured. The involvement of the MEK/ERK signaling pathway was determined. COPD mice exhibited severe lung damage and impaired club cell function. Activation of the TGF-β1/ALK5 and MEK/ERK pathways were observed in COPD mice. However, administration of LY2109761 in COPD mice inactivated the TGF-β1/ALK5 and MEK/ERK pathways. Administration of LY2109761 also alleviated pulmonary fibrosis, downregulated the levels cleaved caspase-3, IL-4, IL-5, IL-13, IL-12, and IFN-γ, and limited the phosphorylation of Chk1. Moreover, LY2109761 enhanced CC16 expression and decreased lung cell apoptosis. Inactivation of the TGF-β1/ALK5 axis inhibits the MEK/ERK signaling pathway, enhances club cell function, and alleviates lung tissue damage. These findings suggest that TGF-β1 is a potential therapeutic target for COPD.

Key words: TGF-β1/ALK5 — MEK/ERK — Club cell — COPD

Abbreviations: ALK5, activator receptor-like kinase 5; BALF, bronchoalveolar lavage fluid; BCA, bicinchoninic acid; BSA, bovine serum albumin; COPD, chronic obstructive pulmonary disease; CSE, cigarette smoke extract; ELISA, enzyme-linked immunosorbent assay ERK, extracellular signal-regulated kinase; MEK, MAP/ERK kinase; NF1, neurofibromatosis genes type 1; NF2, neurofibromatosis genes type 2; TGF-β1, transforming growth factor-β1; TUNEL, terminal deoxyribonucleotide transferase-mediated dUTP nick end labeling.

Correspondence to: Hao Yuan, Pulmonary and Critical Care Medicine, Changsha Fourth Hospital, Changsha, Hunan, 410006 China
E-mail: Yuanhao5105851@163.com

Introduction

Chronic obstructive pulmonary disease (COPD) is a major global cause of mortality and morbidity. It is characterized by progressive expiratory airflow limitation, chronic inflammation, and pulmonary emphysema (Bagdonas et al. 2015). Complications such as respiratory failure and pulmonary heart disease can arise from COPD (Wang L et al. 2020). Common symptoms of COPD include breathlessness, cough, and sputum production (Vogelmeier et al. 2020). With over 3 million deaths worldwide every year, COPD poses a significant health challenge (Rabe and Watz 2017). Enhancing the diagnosis and treatment of COPD and reducing its incidence and mortality rates are of global importance.

Multiple signaling pathways play a role in the development and progression of COPD. In particular, transforming growth factor-β1 (TGF-β1) is closely linked to airway remodeling in COPD (van der Velden et al. 2018). The activin receptor-like kinase 5 (ALK5) is a specific receptor of TGF-β1 and is activated by binding TGF-β to the receptor complex, leading to the phosphorylation and activation of extracellular signal-regulated kinase (ERK) and mitogen-activated protein kinase (MAPK) (Ungefroren et al. 2019). Inhibitors of the mitogen-activated and extracellular signal-regulated kinase (MEK)/ERK signaling pathway have been shown to suppress the production of tumor necrosis factor-alpha (TNF-α) in lipopolysaccharide (LPS)-stimulated macrophages/monocytes and protect mice from LPS-induced endotoxic shock (Chen et al. 2020). TGF-β activates the ERK 1/2 signaling in cancer-associated fibroblasts (CAF), leading to increased production of CAF-derived cardiotrophin-like cytokine factor 1 (CLCF1), which forms a positive feedback loop that contributes to hepatocellular carcinoma progression (Song et al. 2021). Furthermore, TGF-β/Sma- and Mad-related protein (Samd) signaling can regulate the activation of ERK1/2, leading to myocardial fibrosis (Cheng et al. 2021). Inhibition of the ERK1/2-mechanistic target of rapamycin complex 1 (mTORC1) axis has shown potential in improving the fibrotic effects induced by proteinuria and TGF-β in adriamycin-induced glomerular sclerosis (Das et al. 2019). These studies further highlight the intricate relationship between Smad and ERK signaling pathways (Petiti et al. 2015). Based on these findings, we hypothesize that the knockdown of TGF-β1/ALK5 may inhibit the MEK/ERK signaling pathway and mitigate the progression of COPD. However, further experimental validation is required to confirm this hypothesis.

Bronchioles are critically affected in COPD, causing significant damage (Berg and Wright 2016; Wiegman et al. 2020). Club cells, also known as Clara cells or bronchiolar exocrine cells, are non-ciliated cells found in the respiratory epithelium. These cells have the ability to survive, proliferate, and differentiate within a span of 2–4 weeks, allowing for the reconstruction of normal airway epithelial cells. As a result, club cells are considered to be progenitor/stem cells of the bronchial epithelium (Xing et al. 2010). Club cell secretory protein (CCSP), also known as club cell protein 16 (CC16) or CC10, is a 15.8 kDa protein primarily released in the terminal bronchioles, where club cells are located (Almuntashiri et al. 2020). CC16 plays a significant protective role in reducing oxidative stress and inflammation in the respiratory tract, while also serving as a peripheral lung marker to assess the integrity and permeability of lung epithelial cells (Hu et al. 2021). More specifically, CC16 has the potential to be a therapeutic target for COPD (Martinu et al. 2023). Clinical data has shown that CC16 levels are reduced in the circulation, bronchoalveolar lavage fluid (BALF), and airways of COPD patients (Almuntashiri et al. 2020). CC16 limits the development of COPD by alleviating inflammation and pulmonary edema (Laucho-Contreras et al. 2016). These findings highlight the importance of club cells and their produced CC16 in the development of COPD.

There is a negative correlation between TGF-β1 and CC16 levels, indicating that inhibiting TGF-β1 might enhance the activity of club cells (Gu et al. 2021). Hydrogen sulfide therapy has been shown to mitigate COPD induced by cigarette smoke through the inhibition of the TGF-β1/Smad pathway (Wang et al. 2020a). However, it remains unknown whether the TGF-β1/ALK5 pathway impacts the survival of club cells by the MEK/ERK signaling pathway. MEK inhibitors have been utilized to treat COPD and reduce airway inflammation (Kurian et al. 2019). However, it is important to note that both the TGF-β1/ALK5 and MEK/ERK pathways can affect the proliferation and DNA damage of various cell types including neurons (Zhang et al. 2019), breast cancer cells (Li et al. 2009), osteosarcoma, and ovarian and breast cancer cells (Lee et al. 2017). Based on these observations, we have put forth a hypothesis that inhibiting the TGF-β1/ALK5 and MEK/ERK pathways may promote the activity of club cells in COPD.

Therefore, the objective of this study was to establish an *in vivo* mouse model of COPD and investigate whether inhibiting the TGF-β1/ALK5 pathway, which regulates MEK/ERK signaling pathway, influences the survival of club cells and potentially alleviates COPD progression.

Materials and Methods

Construction of COPD model mice

Forty male C57BL/6J mice (25 ± 2 g) were purchased from Hunan Silaikejingda Experimental Animal Co., Ltd. A scheme demonstrating the time management of the experiment was helpful in understanding our work (Fig. 1). In brief, to investigate lung injury and club cell functional changes in COPD, the animals were randomly divided into Normal group and COPD group, with 8 mice in each group. After one week of acclimation, mice were used to establish an

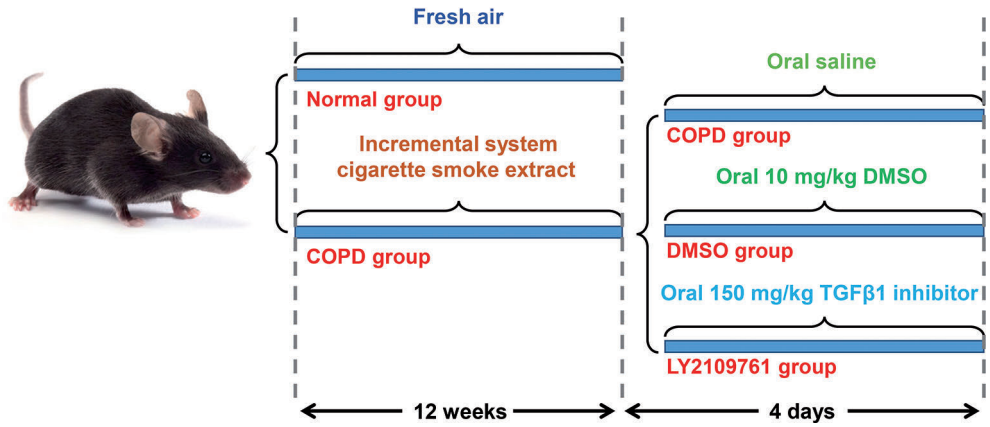

Figure 1. Scheme demonstrating time management of the animal experiments.

in vivo COPD model by exposure to cigarette smoke extract (CSE) (Su et al. 2020). The incremental CSE process started in October 2022 and ended in December of the same year. In brief, COPD mice were placed in a smoking chamber where the smoke from commercial filtered cigarettes (containing 0.8 mg nicotine, 11 mg tar, and 13 mg carbon monoxide *per* cigarette) was introduced. The COPD mice were exposed to 1 h of CSE twice a day (morning and afternoon), for a total of 12 weeks (Ridzuan et al. 2021). The 12-week CSE process was divided into four stages, with the amount of smoke the mice received increasing gradually with the duration of smoking. Throughout the smoke exposure process, carbon monoxide concentration was maintained at 310–380 ppm and oxygen concentration was ≥18%. The mice in Normal group, on the other hand, were continuously kept in fresh air. COPD mice were evaluated as described previously (Su et al. 2020).

To investigate the effects of TGF-β1 on club cell function in COPD, the COPD mice were further divided into COPD group, DMSO group, and LY2109761 group, with 8 mice in each group. After CSE treatment, the mice in DMSO group received oral administration of 10 mg/kg DMSO daily for 4 days. The mice in the LY2109761 group received oral administration of 150 mg/kg TGF-β1 receptor inhibitor LY2109761 daily for 4 days (Wang et al. 2021). LY2109761 was dissolved in DMSO and stored at −80°C. The mice in COPD group received an equal dosage of normal saline by orally once a day for 4 days.

Hemotoxylin-eosin staining

The paraffin-embedded mouse lung tissue was subjected to a roasting process at 60°C for 12 h. Subsequently, the tissue sections were sequentially treated with xylene for dewaxing and gradient ethanol for rehydration. For staining, hematoxylin eosin staining solution (AWI0020a, Abiowell, China) was used. Following staining, the sections were dehydrated with gradient ethanol (95–100%) and then placed in xylene. Finally, the sections were sealed using neutral gum and observed under a light microscope (BA210T, Motic, Germany). Lung injury was blindly scored according to a previous protocol (Cheng et al. 2019). The scoring items included alveolar septa, intrapulmonary hemorrhage, and bronchial inflammation. Each scoring item ranged from 0 to 4, with 0 representing no injury and 4 representing severe lesions.

Terminal deoxyribonucleotide transferase (TdT)-mediated dUTP nick end labeling (TUNEL)

To evaluate apoptosis in the lung tissue of mice, the TUNEL test kit (40306ES50, YEASEN, China) was used according to the corresponding instructions. The cells were then stained with 4',6-diamidino-2-phenylindole (DAPI) staining solution (AWI0331a, Abiowell, China) to visualize the nuclei, and subsequently observed under a light microscope. The apoptotic rate of lung cells was evaluated by calculating the percentage of TUNEL-positive cells to the total number of cells in the region.

Enzyme-linked immunosorbent assay (ELISA)

The procedures of BALF were performed with reference to the previous protocol (Li et al. 2020). After sacrificing the mice, the entire lungs were injected with 4 ml of saline and lavaged three times to obtain the BALF. The levels of interleukin-1beta (IL-1β) (KE10003), IL-6 (KE10007), TNF-α (KE10002), IL-4 (KE10010), IL-5 (KE10018), IL-13 (KE10021), IL-12 (KE10014), and interferon-gamma (IFN-γ) (KE10001) in serum and BALF were detected according to the instructions. All kits used were obtained from Proteintech (USA).

Western blotting

The radioimmunoprecipitation assay (RIPA) lysate (AWB0136, Abiowell, China) was used to isolate total protein samples from lung tissues. The protein concentration was determined using a bicinchoninic acid (BCA) protein

concentration assay kit (ab102536, Abcam, UK) according to the instructions. Subsequently, the proteins were separated by sodium dodecyl sulphate-polyacrylamide gel electrophoresis (SDS-PAGE) and transferred to nitrocellulose membranes. The membranes were sealed using a buffer containing 5% skim milk. Next, the membranes were incubated with the primary antibodies overnight at 4°C, including TGF-β1 (ab215715, Abcam, UK), ALK5 (ab235578, Abcam, UK), p-ALK5 (PA5-40298, ThermoFisher, USA), phosphorylated (p)-MEK (ab96379, Abcam, UK), MEK (ab32091, Proteintech, USA), ERK (16443-1-AP, Proteintech, USA), p-ERK (28733-1-AP, Proteintech, USA), CC16 (ab213203, Abcam, UK), checkpoint kinase 1 (Chk1) (25887-1-AP, Proteintech, USA), p-Chk1(28805-1-AP, Proteintech, USA), Caspase3 (#9661, CST, USA), and β-actin (66009-1-Ig, Proteintech, USA). Following that, the membranes were co-incubated with HRP goat anti-mouse IgG (SA00001-1, Proteintech, USA) and HRP goat anti-rabbit IgG (SA00001-2, Proteintech, USA) at room temperature for 90 min. After that, the membranes were incubated with an enhanced chemiluminescence (ECL) solution (AWB0005, Abiowell, China) for 1 min and the protein bands were detected using ChemiScope6100 (CLiNX, China). The relative protein levels were determined by calculating the gray value of the corresponding protein band relative to the gray value of the β-actin protein band.

Immunohistochemistry staining

After being roasted at 60°C for 12 h, the lung sections were dewaxed and rehydrated successively in xylene and gradient ethanol. To repair the antigen, 0.01 M citrate buffer (pH 6.0) was used at high temperatures. Next, 1% periodate was added to inactivate endogenous enzymes. The primary antibodies (CC16, 10490-1-AP, 1:200, Proteintech, USA; Caspase3, 19677-1-AP, 1:200, Proteintech, USA) were incubated with samples overnight at 4°C. Subsequently, the secondary antibodies were co-incubated with samples at 37°C for 30 min. After color rendering using diaminobenzidine (DAB) and re-staining with hematoxylin, the sections were dehydrated once again. Finally, the sections were immersed in xylene, sealed with neutral gum, and observed under a microscope.

Immunofluorescence

The lung tissues from mice were roasted at 60°C for 12 h. Subsequently, they were subjected to dewaxing and rehydration by being placed in xylene and gradient ethanol. Thermal antigen retrieval was performed on lung tissue sections, followed by treatment with sodium borohydride solution, 75% ethanol solution, and Sudan black dye solution for specific durations. Then, the sections were treated with 5% bovine serum albumin (BSA) for 60 min to block non-specific binding. The tissue samples were then incubated overnight at 4°C with the gamma-H2A histone family member (γ-H2AX) antibody (13584-1-AP, Abcam, UK). Subsequently, the samples were incubated with a fluorescently labeled goat anti-rabbit IgG(H+L) secondary antibody (SA00013-2, Proteintech, USA) at 37°C for 90 min. Nuclei were stained with DAPI (AWC0293a, Abiowell, China) at 37°C for 10 min. Finally, the sections were observed under a microscope after being encapsulated in glycerin.

Masson trichrome staining

The lung tissues from mice underwent a roasting process at 60°C for 12 h. According to the instructions of the Masson staining kit (AWI0253, Abiowell, China), the sections were dewaxed to water and stained with the nuclear dye solution for 1 min. Subsequently, the sections were immersed in distilled water and ammonia for 10 min to restore the nuclei to blue. Next, the slurry dye was added and allowed to stain for 5 min. A color separation solution was applied for approximately 30 s to separate the colors. Then, a redye solution was added to cover the entire tissue for 8 min. Finally, the sections were rendered transparent using the xylene, sealed with neutral gum, and observed using a light microscope.

Statistical analysis

Data were presented as mean ± standard deviation, and each experiment was repeated at least 3 times. Statistical analysis was performed using GraphPad Prism 9.0. Student's *t*-test was used to compare between two groups, while one-ANOVA or two-ANOVA was used for comparison among multiple groups. $p < 0.05$ was considered statistically significant.

Results

Construction of a mouse model of COPD

In the Normal group, the alveolar structure appeared intact with no evident inflammatory infiltration. Compared to the healthy mice, COPD mice exhibited deformity of alveolar structure, thickening of alveolar walls, reduced alveolar spaces, interstitial edema, and significant inflammatory infiltrates (Fig. 2A). COPD mice had higher scores compared to Normal group (Fig. 2B), indicating severe lung injury in COPD mice. The apoptosis rate in COPD group was higher compared to Normal group (Fig. 2C). Additionally, the levels of IL-1β, IL-6, and TNF-α were significantly increased in COPD group compared to Normal group (Fig. 2D). Compared to Normal group, COPD group showed markedly elevated levels of TGF-β1 and ALK5, as well as enhanced phosphorylation levels of MEK and ERK (Fig. 2E). Taken together, these results demonstrated the successful establishment of the COPD mice model.

COPD mice exhibited impaired club cell function and lung injury

To assess the survival of club cells and the extent of tissue cell injury in the COPD mice, we evaluated the expression of CC16, a protein associated with club cell function, as well as the DNA damage marker γ-H2AX, the apoptotic marker cleaved Caspase3, and the DNA damage response protein Chk1. We observed a notable decrease in the level of CC16 protein in COPD group compared to Normal group

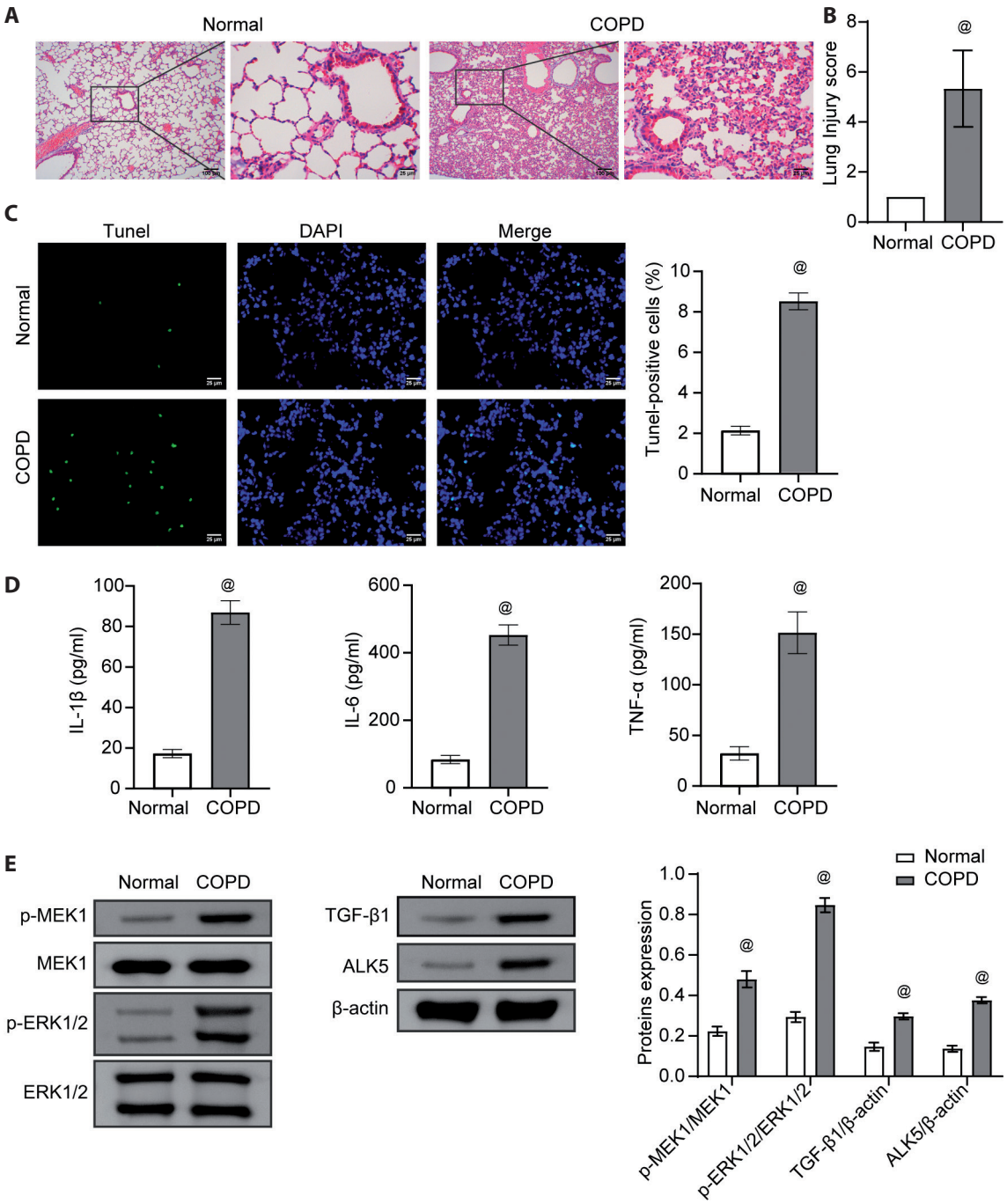

Figure 2. Construction of the COPD mice model. **A.** Hemotoxylin-eosin staining was used to detect the damage to mouse lung tissue. **B.** The lung injury scores of each group of mice were recorded. **C.** Apoptosis was detected by TUNEL staining. **D.** The levels of inflammatory cytokines, including IL-1β, IL-6, and TNF-α, in serum were determined by ELISA. **E.** The levels of TGF-β1, ALK5, MEK, p-MEK, ERK, and p-ERK were detected by Western blotting. $^{@}$ $p < 0.05$ *vs*. Normal group.

(Fig. 3A). The positive expression of CC16 was significantly lower in COPD group (Fig. 3B). These results indicated that club cell survival was impaired in COPD mice. Conversely, the expression of γ-H2AX was higher in COPD group compared to Normal group (Fig. 3C). Moreover, the levels of cleaved Caspase3 and the phosphorylation levels of Chk1 were elevated in COPD group compared to Normal group (Fig. 3D). The results collectively suggested that the survival of club cells was reduced and tissue cell damage was increased in COPD mice.

TGF-β1 knockdown regulated the MEK/ERK signaling pathway

To investigate the relationship between the TGF-β1/ALK5 and MEK/ERK signaling pathways, we used a TGF-β1 inhibitor, LY2109761, to knockdown its expression in COPD mice. Compared to DMSO group, the levels of TGF-β1 and the phosphorylation levels of ALK5, MEK, and ERK were reduced in LY2109761 group (Fig. 4). These findings suggested that TGF-β1 knockdown limited the TGF-β1/ALK5 and MEK/ERK signaling pathways.

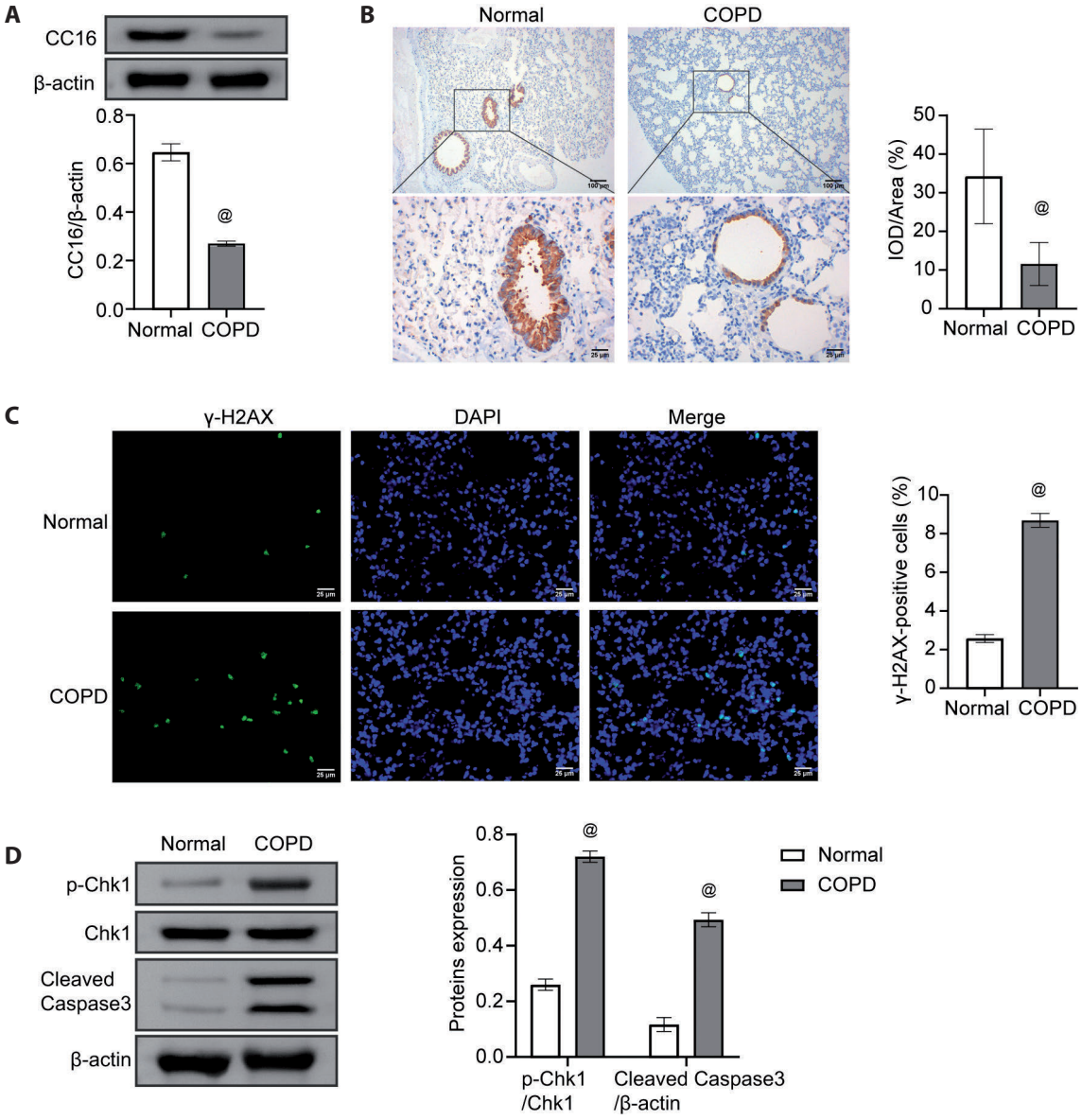

Figure 3. Club cell survival and lung damage were assessed in COPD mice. **A.** The expression of CC16 was measured by Western blotting. **B.** Immunohistochemistry staining was utilized to measure the positive expression of CC16. **C.** The levels of γ-H2AX were detected using immunofluorescence assays. **D.** The levels of cleaved Caspase3, Chk1, and p-Chk1 were detected using Western blotting. $^{@}$ $p < 0.05$ *vs.* Normal group.

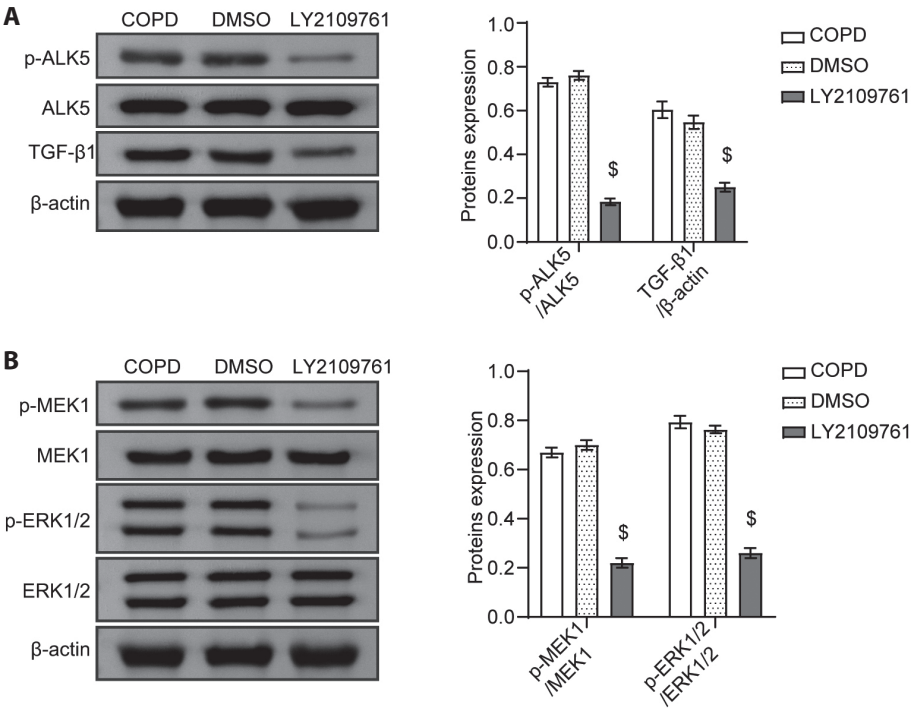

Figure 4. TGFβ1/ALK5 regulated the MEK/ERK signaling pathway. The levels of TGF-β1, ALK5, p-ALK5 (**A**) and the levels of MEK, p-MEK, ERK, p-ERK (**B**) were detected by Western blotting. $^{\$}$ $p < 0.05$ *vs.* DMSO group.

Inactivation of the TGF-β1/ALK5 signaling pathway mitigated lung injury in COPD mice

To further confirm the regulatory function of TGF-β1/ALK5 and MEK/ERK signaling pathways in the tissue injury of mice with COPD, we assessed the pathological conditions of lung tissue, the level of impaired apoptosis, and the changes in related inflammatory factors in mice. In COPD group, pulmonary fibrosis was observed to be severe. However, after administration with LY2109761, the extent of fiber deposition in the lungs of the mice was noticeably inhibited in COPD mice (Fig. 5A). The positive rate of Caspase3 was decreased in lung tissues of mice after administration with LY2109761 (Fig. 5B). Additionally, the levels of IL-4, IL-5, IL-13, IL-12, and IFN-γ in the BALF were remarkably reduced in LY2109761 group (Fig. 5C). These results indicated that inhibiting the expression of TGF-β1 effectively improved pulmonary fibrosis, delayed cell apoptosis, and decreased the levels of inflammatory factors such as IL-4, IL-5, IL-13, IL-12, and IFN-γ in the BALF.

Inactivation of the TGF-β1/ALK5 signaling pathway enhanced the activity of club cell in COPD mice

To validate the effects of the TGF-β1/ALK5 signaling pathway on club cell activity in COPD mice, we assessed the expression of CC16 and cleaved Caspase3 as well as apoptosis. Compared to DMSO group, the positive expression level of CC16 was dramatically increased, while the apoptosis rate was markedly decreased in LY2109761 group (Fig. 6A). Additionally, the levels of cleaved Caspase3 and p-Chk1 were downregulated in COPD mice after administration with LY2109761 (Fig. 6B). These results indicated that inactivation of the TGF-β1/ALK5 signaling pathway restored club cell dysfunction and inhibited cell apoptosis in COPD mice.

Discussion

Studies have reported that long-term exposure to smoke can cause physical and chemical stimulation to the respiratory tract, which can lead to airway mucosal damage and chronic inflammation, ultimately resulting in reduced airway function and the development of COPD (Kim et al. 2008). The role of mast cell trypsin in the pathogenesis of COPD has been identified using a mouse model of COPD (Beckett et al. 2013). It was reported that smoke exposure could be used to establish the rat model of COPD skeletal muscle dysfunction (Su et al. 2020). In this study, mice exposed to smoke showed pulmonary edema, bronchitis, and increased lung cell apoptosis, suggesting a successful COPD model. Therefore, we used the established COPD model for follow-up studies.

Studies have demonstrated that CC16 can effectively protect alveolar epithelium, prevent harmful substances from destroying lung tissue, and enhance lung immune function (Iannuzzi 2004). Reduction of club cell protein is considered a key indicator of early epithelial damage caused by tobacco smoke (Cuzić et al. 2012). Research has shown that serum

CC16 levels in smokers are lower compared to those in former smokers, and both smokers and former smokers are markedly lower compared to those in individuals who have never smoked (Lomas et al. 2008). Additionally, studies have observed a significant inhibition of airway CC16 expression in COPD patients, smoke-exposed monkey models, and smoke-induced COPD mouse models. The loss of CC16 expression has been associated with aggravated airway inflammation and alveolar damage in mice (Zhu et al. 2015). In our study, we observed negative expression of CC16 in COPD group, indicating impaired survival of club cells in COPD mice. Furthermore, the levels of γ-H2AX, cleaved Caspase3, and phosphorylated Chk1 were significantly increased in COPD mice. An increased number of γ-H2AX foci, elevated phosphorylation of Chk1, and higher levels of cleaved Caspase3 are indicators of DNA damage and

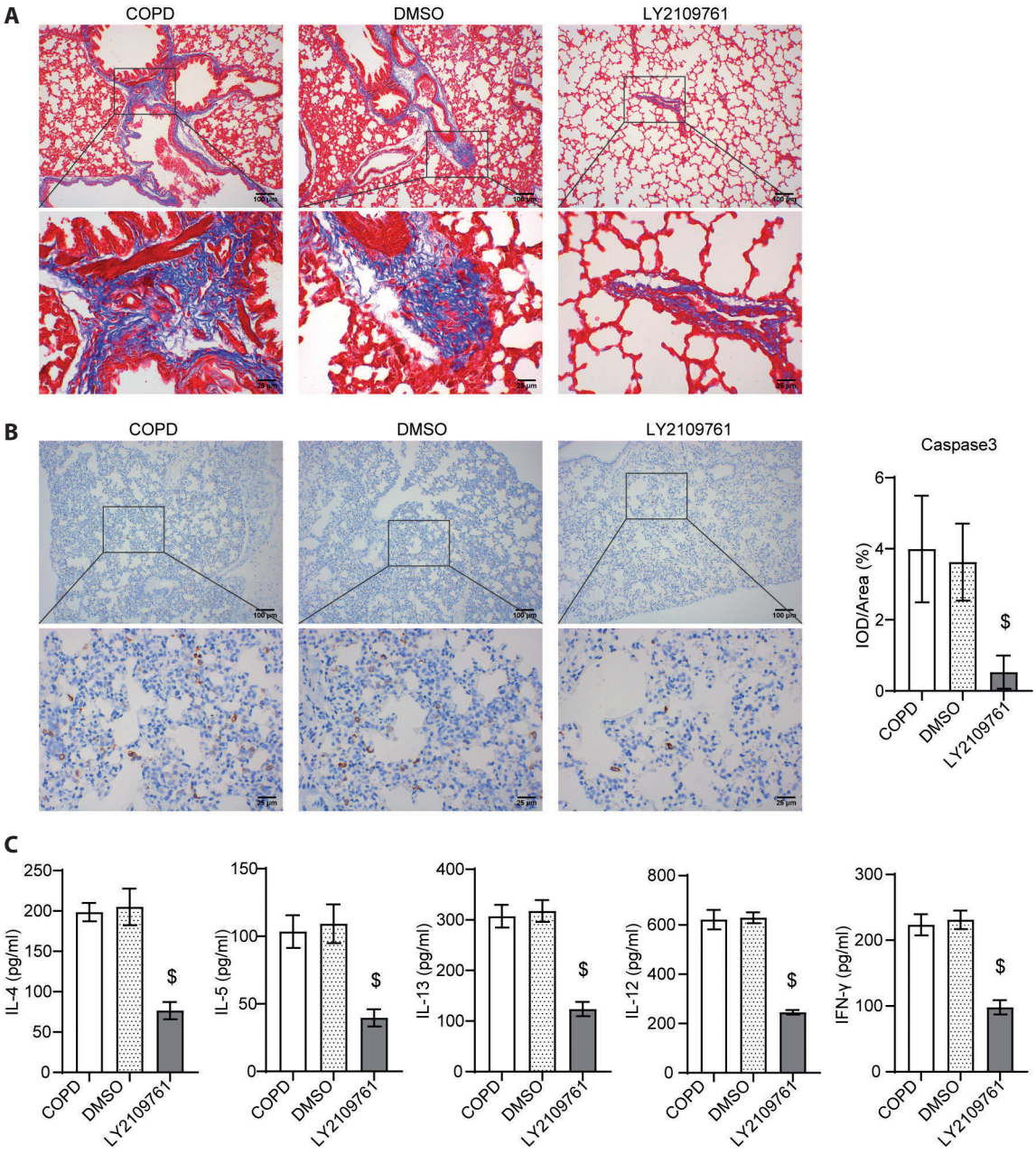

Figure 5. TGFβ1/ALK5 modulated the MEK/ERK signaling pathway to improve chronic obstructive pulmonary injury in mice. **A.** The degree of pulmonary fibrosis was assessed by Masson staining. **B.** Positive rate of Caspase3 was examined by immunohistochemistry staining. **C.** The levels of IL-4, IL-5, IL-13, IL-12, and IFN-γ in BALF were determined by ELISA. $^{\$}$ $p < 0.05$ *vs*. DMSO group.

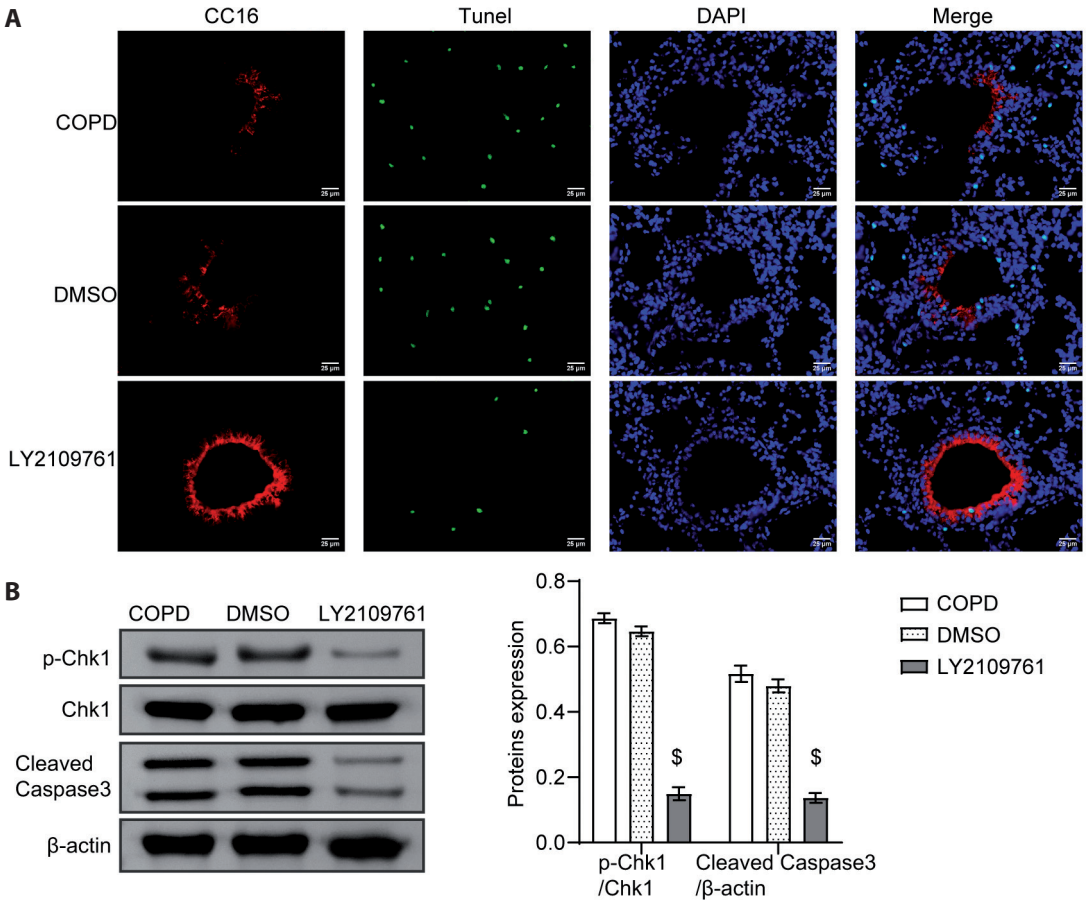

Figure 6. Effect of TGFβ1/ALK5 on the activity of club cells in COPD mice. **A.** TUNEL double staining was used to label CC16-positive and apoptotic cells. **B.** The levels of cleaved Caspase3, Chk1, and p-Chk1 were detected by Western blotting. $^{\$}$ $p < 0.05$ *vs.* DMSO group.

apoptosis (Campagne et al. 2020; Klomp et al. 2021). These results suggested that the lung tissue of COPD mice in our study experienced aggravated cell damage. Taken together, our results indicate decreased survival of club cells and increased tissue cell damage in COPD mice.

Furthermore, TGF-β1 is a multifunctional cytokine with noticeably increased plasma levels in COPD patients (Mak et al. 2009). Increased T-cell apoptosis in the airway of COPD patients resulted in unbalanced cell homeostasis, defective clearance of apoptotic substances by monocytes/macrophages, secondary necrosis, and prolonged inflammatory responses, which is closely associated with activated TGF-β1 signaling (Hodge et al. 2003). Our research found that the TGF-β1/ALK5 and signaling pathway was activated in COPD mice. We also observed activated MEK/ERK signaling pathway in COPD mice. The MEK/ERK signaling pathway plays an important role in the development of many types of cancer (Ullah et al. 2022). Studies have shown that activation of the Raf/MEK/ERK pathway promotes the progression of colorectal cancer (Wang X et al. 2020). Activated ERK pathway is also found in other types of cancer, including breast cancer (Jin et al. 2019), nasopharynx cancer (Ding et al. 2022), and pancreatic cancer (Li et al. 2022). Inhibition of the MEK1/ERK signaling pathway has been demonstrated to effectively inhibit tumor growth and metastasis (Du et al. 2022). It has also been demonstrated that TGF-β1-induced keratinocyte motility is associated with the MEK/ERK signaling pathway (Feng et al. 2022). However, the relationship between TGF-β1 and MEK/ERK in COPD had not been reported. In this study, we found that in COPD mice, the TGF-β1/ALK5 and MEK/ERK signaling pathways were activated. The levels of TGF-β1 and the phosphorylation level of ERK, MEK, and ALK5 in lung tissues were decreased in COPD mice after administration with a TGF-β1 inhibitor. LY2109761 disrupted the binding of ALK5 to TGF-β1, resulting in decreased phosphorylation levels of MEK, ERK, and ALK5. These findings suggested that inactivation of the TGF-β1/ALK5 axis inhibited the MEK/ERK signaling pathway.

The MEK/ERK pathway has been identified as a potential therapeutic target for cancer treatment, as knockdown of

MEK/ERK has shown to inhibit kidney injury and renal fibrosis (Barbosa et al. 2021). Moreover, MEK1/2 inhibitors have been proposed as potential treatments for lesions caused by pathogenic variants of neurofibromatosis genes type 1 and type 2 (NF1, NF2) (Harder 2021). On the other hand, impaired TGF-β signaling has been linked to accelerated inflammation and the development of COPD (Zhang et al. 2016). CC16 directly inhibits the production and activity of IFN-γ, TNF-α, IL-1β, and other inflammatory mediators, limiting the inflammatory cascade reaction (Broeckaert and Bernard 2000). Increased levels of IL-1β, TNF-α and TGF-β1 are observed in COPD rats (Li et al. 2014). However, the specific role of the TGF-β1/ALK5 and MEK/ERK signaling pathways in COPD had not been established. In our study, we observed that COPD group exhibited severe pulmonary fibrosis, which was reduced after inhibiting the expression of TGF-β1. In addition, administration with LY2109761 led to a decrease in the positive rate of Caspase3, as well as reduced levels of IL-4, IL-5, IL-13, IL-12 and IFN-γ. These findings supported the effectiveness of regulating the TGF-β1/ALK5 axis in improving lung fibrosis, delaying lung cell apoptosis, and reducing the expression of pro-inflammatory factors in the BALF. These results suggested that the regulation of TGF-β1/ALK5, and its impact on the MEK/ERK signaling pathway, mitigated tissue injury associated with COPD in mice.

Previous studies have indicated that TGF-β1 can stimulate the generation of club cells by binding to the ALK5 receptor, with ALK5 playing a vital role in this process. The deletion of ALK5 has been shown to impact the development of bronchial epithelial progenitor cells, resulting in a significant decrease in the expression level of club cell protein (Xing et al. 2010). In our study, we further investigated the effect of TGF-β1/ALK5 on the activity of club cells in COPD mice by inhibiting the expression of TGF-β1. Our results demonstrated that COPD mice treated with LY2109761 exhibited downregulated phosphorylation levels of MEK and ERKl, lower levels of cleaved Caspase3, decreased apoptosis rate, and increased levels of CC16. These above results showed that the TGF-β1/ALK5 pathway has a significant impact on the activity of club cells in COPD mice.

Limitations of the study

We acknowledge that our study has certain limitations. One limitation is that the different groups did not select lung tissue from the same site for hemotoxylin-eosin staining, TUNEL, Western blotting, and other experiments. Further standardization and refinement of the study regions in each group is necessary to minimize interference from other factors. Additionally, we have yet to demonstrate the clinical-level impact of TGF-β1/ALK5 regulation on the MEK/ERK signaling pathway, club cell activity, and lung tissue damage improvement in COPD. Therefore, we eagerly anticipate expanding our research to the clinical level in future studies.

Conclusion

In this study, we have made advancements in understanding the mechanism of club cell-related pathways and factors in COPD. Our research has provided innovative insights into the theoretical aspects of this field. Moreover, we have demonstrated the potential of inhibiting the TGF-β1/ALK5 pathway, which regulates the MEK/ERK signaling pathway, to improve club cell survival and inhibit the development of COPD. Our study has laid the foundation for further elucidating the pathogenesis of COPD and has proposed a novel idea for the development of targeted drugs for its treatment.

Funding. This study was supported by Changsha Natural Science Foundation (kq2202019).

Conflicts of interest. All authors have completed the ICMJE uniform disclosure form. The authors have no conflicts of interest to declare.

Availability of data and materials. All raw data are available from the corresponding author if necessary.

Author contributions. JT and HY was responsible for conception and design. JT, HO, JW, LW, and XL analyzed and interpreted the data, or analysis and interpretation of data, JT and FY was a major contributor in writing the manuscript. All authors read and approved the final manuscript.

Ethics approval and consent to participate. The animal experiment was approved by Animal Ethics Committee of Changsha Fourth Hospital (No. CSSDSYY-LLSC-KYXM-2022-3-5).

References

Almuntashiri S, Zhu Y, Han Y, Wang X, Somanath P, Zhang D (2020): Club cell secreted protein cc16: potential applications in prognosis and therapy for pulmonary diseases. J. Clin. Med. **9,** 4039 https://doi.org/10.3390/jcm9124039

Bagdonas E, Raudoniute J, Bruzauskaite I, Aldonyte R (2015): Novel aspects of pathogenesis and regeneration mechanisms in COPD. Int. J. Chron. Obstruct. Pulmon. Dis. **10,** 995-1013 https://doi.org/10.2147/COPD.S82518

Barbosa R, Acevedo L, Marmorstein R (2021): The MEK/ERK network as a therapeutic target in human cancer. Mol. Cancer Res. **19,** 361-374 https://doi.org/10.1158/1541-7786.MCR-20-0687

Beckett EI, Stevens RI, Jarnicki AG, Kim RY, Hanish I, Hansbro NG, Deane A, Keely S, Horvat JC, Yang M, et al. (2013): A new short-term mouse model of chronic obstructive pulmonary disease identifies a role for mast cell tryptase in pathogenesis. J. Allergy Clin. Immunol. **131,** 752-762

https://doi.org/10.1016/j.jaci.2012.11.053
Berg K, Wright JL (2016): The pathology of chronic obstructive pulmonary disease: progress in the 20th and 21st centuries. Arch. Pathol. Lab. Med. **140,** 1423-1428 https://doi.org/10.5858/arpa.2015-0455-RS
Broeckaert F, Bernard A (2000): Clara cell secretory protein (CC16): characteristics and perspectives as lung peripheral biomarker. Clin. Exp. Allergy **30,** 469-475 https://doi.org/10.1046/j.1365-2222.2000.00760.x
Campagne O, Davis A, Maharaj AR, Zhong B, Stripay J, Farmer D, Roussel MF, Stewart CF (2020): CNS penetration and pharmacodynamics of the CHK1 inhibitor prexasertib in a mouse Group 3 medulloblastoma model. Eur. J. Pharm. Sci. **142,** 105106 https://doi.org/10.1016/j.ejps.2019.105106
Chen H, Chen H, Liang J, Gu X, Zhou J, Xie C, Lv X, Wang R, Li Q, Mao Z, et al. (2020): TGF-β1/IL-11/MEK/ERK signaling mediates senescence-associated pulmonary fibrosis in a stress-induced premature senescence model of Bmi-1 deficiency. Exp. Mol. Med. **52,** 130-151 https://doi.org/10.1038/s12276-019-0371-7
Cheng Q, Fang L, Feng D, Tang S, Yue S, Huang Y, Han J, Lan J, Liu W, Gao L, Luo Z (2019): Memantine ameliorates pulmonary inflammation in a mice model of COPD induced by cigarette smoke combined with LPS. Biomed. Pharmacother. **109,** 2005-2013 https://doi.org/10.1016/j.biopha.2018.11.002
Cheng X, Wang L, Wen X, Gao L, Li G, Chang G, Qin S, Zhang D (2021): TNAP is a novel regulator of cardiac fibrosis after myocardial infarction by mediating TGF-β/Smads and ERK1/2 signaling pathways. EBioMedicine **67,** 103370 https://doi.org/10.1016/j.ebiom.2021.103370
Cuzić S, Bosnar M, Kramarić MD, Ferencić Z, Marković D, Glojnarić I, Eraković Haber V (2012): Claudin-3 and Clara cell 10 kDa protein as early signals of cigarette smoke-induced epithelial injury along alveolar ducts. Toxicol. Pathol. **40,** 1169-1187 https://doi.org/10.1177/0192623312448937
Das R, Kim SJ, Nguyen NT, Kwon HJ, Cha SK, Park KS (2019): Inhibition of the ERK1/2-mTORC1 axis ameliorates proteinuria and the fibrogenic action of transforming growth factor-β in Adriamycin-induced glomerulosclerosis. Kidney Int. **96,** 927-941 https://doi.org/10.1016/j.kint.2019.05.006
Ding S, Gao Y, Lv D, Tao Y, Liu S, Chen C, Huang Z, Zheng S, Hu Y, Chow LK, et al. (2022): DNTTIP1 promotes nasopharyngeal carcinoma metastasis via recruiting HDAC1 to DUSP2 promoter and activating ERK signaling pathway. EBioMedicine **81,** 104100 https://doi.org/10.1016/j.ebiom.2022.104100
Du J, Lan T, Liao H, Feng X, Chen X, Liao W, Hou G, Xu L, Feng Q, Xie K, et al. (2022): CircNFIB inhibits tumor growth and metastasis through suppressing MEK1/ERK signaling in intrahepatic cholangiocarcinoma. Mol. Cancer **21,** 18 https://doi.org/10.1186/s12943-021-01482-9
Feng X, Feng W, Ji Y, Jin T, Li J, Guo J (2022): Transforming growth factor-beta1 negatively regulates SOCS7 via EGR1 during wound healing. Cell Commun. Signal. **20,** 86 https://doi.org/10.1186/s12964-022-00893-5
Gu Y, He W, Wang Y, Chen J, Wang H, Gao P, Yang S, Zhu X, Ma W, Li T (2021): Respiratory effects induced by occupational exposure to refractory ceramic fibers. J. Appl. Toxicol. **41,** 421-441 https://doi.org/10.1002/jat.4053
Harder A (2021): MEK inhibitors – novel targeted therapies of neurofibromatosis associated benign and malignant lesions. Biomark Res. **9,** 26 https://doi.org/10.1186/s40364-021-00281-0
Hodge SJ, Hodge GL, Reynolds PN, Scicchitano R, Holmes M (2003): Increased production of TGF-beta and apoptosis of T lymphocytes isolated from peripheral blood in COPD. Am. J. Physiol. Lung Cell Mol. Physiol. **285,** L492-499 https://doi.org/10.1152/ajplung.00428.2002
Hu T, Sun F, Yu X, Li Q, Zhao L, Hao W, Han W (2021): CC16-TNF-α negative feedback loop formed between Clara cells and normal airway epithelial cells protects against diesel exhaust particles exposure-induced inflammation. Aging (Albany NY) **13,** 19442-19459 https://doi.org/10.18632/aging.203356
Iannuzzi MC (2004): Clara cell protein in sarcoidosis: another job for the respiratory tract protector? Am. J. Respir. Crit. Care Med. **169,** 143-144 https://doi.org/10.1164/rccm.2311002
Jin X, Li Y, Guo Y, Jia Y, Qu H, Lu Y, Song P, Zhang X, Shao Y, Qi D, et al. (2019): ERα is required for suppressing OCT4-induced proliferation of breast cancer cells via DNMT1/ISL1/ERK axis. Cell Prolif. **52,** e12612 https://doi.org/10.1111/cpr.12612
Kim V, Rogers TJ, Criner GJ (2008): New concepts in the pathobiology of chronic obstructive pulmonary disease. Proc. Am. Thorac. Soc. **5,** 478-485 https://doi.org/10.1513/pats.200802-014ET
Klomp JE, Lee YS, Goodwin CM, Papke B, Klomp JA, Waters AM, Stalnecker CA, Deliberty JM, Drizyte-Miller K, Yang R, et al. (2021): CHK1 protects oncogenic KRAS-expressing cells from DNA damage and is a target for pancreatic cancer treatment. Cell Rep. **37,** 110060 https://doi.org/10.1016/j.celrep.2021.110060
Kurian N, Cohen TS, Öberg L, De Zan E, Skogberg G, Vollmer S, Baturcam E, Svanberg P, Bonn B, Smith PD, et al. (2019): Dual role for a MEK inhibitor as a modulator of inflammation and host defense mechanisms with potential therapeutic application in COPD. Int. J. Chron. Obstruct. Pulmon. Dis. **14,** 2611-2624 https://doi.org/10.2147/COPD.S211619
Laucho-Contreras ME, Polverino F, Tesfaigzi Y, Pilon A, Celli BR, Owen CA (2016): Club cell protein 16 (CC16) augmentation: A potential disease-modifying approach for chronic obstructive pulmonary disease (COPD). Expert Opin. Ther. Targets **20,** 869-883 https://doi.org/10.1517/14728222.2016.1139084
Lee HJ, Cao Y, Pham V, Blackwood E, Wilson C, Evangelista M, Klijn C, Stokoe D, Settleman J (2017): Ras-MEK signaling mediates a critical Chk1-dependent DNA damage response in cancer cells. Mol. Cancer Ther. **16,** 694-704 https://doi.org/10.1158/1535-7163.MCT-16-0504
Li H, Sekine M, Seng S, Avraham S, Avraham HK (2009): BRCA1 interacts with Smad3 and regulates Smad3-mediated TGF-beta signaling during oxidative stress responses. PLoS One **4,** e7091 https://doi.org/10.1371/journal.pone.0007091

Li H, Yan X, Feng S, Li S, Zhang H, Li J, Qi T (2020): Antagonism of interleukin 17 protects chronic obstructive pulmonary disease rat lungs from adverse effects of environmental PM2.5. Am. J. Transl. Res. **12,** 5808-5817

Li J, Song Y, Zhang C, Wang R, Hua L, Guo Y, Gan D, Zhu L, Li S, Ma P, et al. (2022): TMEM43 promotes pancreatic cancer progression by stabilizing PRPF3 and regulating RAP2B/ERK axis. Cell. Mol. Biol. Lett. **27,** 24 https://doi.org/10.1186/s11658-022-00321-z

Li Y, Li JS, Li WW, Li SY, Tian YG, Lu XF, Jiang SL, Wang Y (2014): Long-term effects of three Tiao-Bu Fei-Shen therapies on NF-κB/TGF-β1/smad2 signaling in rats with chronic obstructive pulmonary disease. BMC Complement. Altern. Med. **14,** 140 https://doi.org/10.1186/1472-6882-14-140

Lomas DA, Silverman EK, Edwards LD, Miller BE, Coxson HO, Tal-Singer R (2008): Evaluation of serum CC-16 as a biomarker for COPD in the ECLIPSE cohort. Thorax **63,** 1058-1063 https://doi.org/10.1136/thx.2008.102574

Mak JC, Chan-Yeung MM, Ho SP, Chan KS, Choo K, Yee KS, Chau CH, Cheung AH, Ip MS (2009): Elevated plasma TGF-beta1 levels in patients with chronic obstructive pulmonary disease. Respir. Med. **103,** 1083-1089 https://doi.org/10.1016/j.rmed.2009.01.005

Martinu T, Todd JL, Gelman AE, Guerra S, Palmer SM (2023): Club cell secretory protein in lung disease: emerging concepts and potential therapeutics. Ann. Rev. Med. **74,** 427-441 https://doi.org/10.1146/annurev-med-042921-123443

Petiti JP, Sosa Ldel V, Sabatino ME, Vaca AM, Gutiérrez S, De Paul AL, Torres AI (2015): Involvement of MEK/ERK1/2 and PI3K/Akt pathways in the refractory behavior of GH3B6 pituitary tumor cells to the inhibitory effect of TGFβ1. Endocrinology **156,** 534-547 https://doi.org/10.1210/en.2014-1070

Rabe KF, Watz H (2017): Chronic obstructive pulmonary disease. Lancet **389,** 1931-1940 https://doi.org/10.1016/S0140-6736(17)31222-9

Ridzuan N, Zakaria N, Widera D, Sheard J, Morimoto M, Kiyokawa H, Mohd Isa SA, Chatar Singh GK, Then KY, Ooi GC, Yahaya BH (2021): Human umbilical cord mesenchymal stem cell-derived extracellular vesicles ameliorate airway inflammation in a rat model of chronic obstructive pulmonary disease (COPD). Stem Cell Res. Ther. **12,** 54 https://doi.org/10.1186/s13287-020-02088-6

Song M, He J, Pan QZ, Yang J, Zhao J, Zhang YJ, Huang Y, Tang Y, Wang Q, He J, et al. (2021): Cancer-associated fibroblast-mediated cellular crosstalk supports hepatocellular carcinoma progression. Hepatology **73,** 1717-1735 https://doi.org/10.1002/hep.31792

Su J, Li J, Lu Y, Li N, Li P, Wang Z, Wu W, Liu X (2020): The rat model of COPD skeletal muscle dysfunction induced by progressive cigarette smoke exposure: a pilot study. BMC Pulm. Med. **20,** 74 https://doi.org/10.1186/s12890-020-1109-y

Ullah R, Yin Q, Snell AH, Wan L (2022): RAF-MEK-ERK pathway in cancer evolution and treatment. Semin. Cancer Biol. **85,** 123-154 https://doi.org/10.1016/j.semcancer.2021.05.010

Ungefroren H, Otterbein H, Fiedler C, Mihara K, Hollenberg MD, Gieseler F, Lehnert H, Witte D (2019): RAC1B suppresses TGF-β1-dependent cell migration in pancreatic carcinoma cells through inhibition of the TGF-β type I receptor ALK5. Cancers (Basel) **11,** 691 https://doi.org/10.3390/cancers11050691

Van Der Velden JL, Wagner DE, Lahue KG, Abdalla ST, Lam YW, Weiss DJ, Janssen-Heininger YMW (2018): TGF-β1-induced deposition of provisional extracellular matrix by tracheal basal cells promotes epithelial-to-mesenchymal transition in a c-Jun NH(2)-terminal kinase-1-dependent manner. Am. J. Physiol. Lung Cell Mol. Physiol. **314,** L984-l997 https://doi.org/10.1152/ajplung.00053.2017

Vogelmeier CF, Román-Rodríguez M, Singh D, Han MK, Rodríguez-Roisin R, Ferguson GT (2020): Goals of COPD treatment: Focus on symptoms and exacerbations. Respir. Med. **166,** 105938 https://doi.org/10.1016/j.rmed.2020.105938

Wang F, Zhang C, Kwagh J, Strassle B, Li J, Huang M, Song Y, Lehman B, Westhouse R, Palanisamy K, et al. (2021): TGFβ2 and TGFβ3 mediate appropriate context-dependent phenotype of rat valvular interstitial cells. iScience **24,** 102133 https://doi.org/10.1016/j.isci.2021.102133

Wang L, Meng J, Wang C, Yang C, Wang Y, Li Y, Li Y (2020): Hydrogen sulfide alleviates cigarette smoke-induced COPD through inhibition of the TGF-β1/smad pathway. Exp. Biol. Med. (Maywood) **245,** 190-200 https://doi.org/10.1177/1535370220904342

Wang X, Wu F, Wang H, Duan X, Huang R, Tuersuntuoheti A, Su L, Yan S, Zhao Y, Lu Y, et al. (2020): PDCD6 cooperates with C-Raf to facilitate colorectal cancer progression via Raf/MEK/ERK activation. J. Exp. Clin. Cancer Res. **39,** 147 https://doi.org/10.1186/s13046-020-01632-9

Wiegman CH, Li F, Ryffel B, Togbe D, Chung KF (2020): Oxidative stress in ozone-induced chronic lung inflammation and emphysema: a facet of chronic obstructive pulmonary disease. Front. Immunol. **11,** 1957 https://doi.org/10.3389/fimmu.2020.01957

Xing Y, Li C, Li A, Sridurongrit S, Tiozzo C, Bellusci S, Borok Z, Kaartinen V, Minoo P (2010): Signaling via Alk5 controls the ontogeny of lung Clara cells. Development **137,** 825-833 https://doi.org/10.1242/dev.040535

Zhang JC, Chen G, Chen L, Meng ZJ, Xiong XZ, Liu HJ, Jin Y, Tao XN, Wu JH, Sun SW (2016): TGF-β/BAMBI pathway dysfunction contributes to peripheral Th17/Treg imbalance in chronic obstructive pulmonary disease. Sci. Rep. **6,** 31911 https://doi.org/10.1038/srep31911

Zhang K, Zhang Q, Deng J, Li J, Li J, Wen L, Ma J, Li C (2019): ALK5 signaling pathway mediates neurogenesis and functional recovery after cerebral ischemia/reperfusion in rats via Gadd45b. Cell Death Dis. **10,** 360 https://doi.org/10.1038/s41419-019-1596-z

Zhu L, Di PY, Wu R, Pinkerton KE, Chen Y (2015): Repression of CC16 by cigarette smoke (CS) exposure. PLoS One **10,** e0116159 https://doi.org/10.1371/journal.pone.0116159

Received: August 15, 2023
Final version accepted: October 16, 2023